Generalized random-phase approximation in the theory of strongly correlated systems

1992 J. Phys.: Condens. Matter 4 9955

(http://iopscience.iop.org/0953-8984/4/49/023)

J. Phys.: Condens. Matter 4 (1992) 9955–9970. Printed in the UK

Generalized random-phase approximation in the theory of strongly correlated systems

Yu A Izyumov, B M Letfulov and E V Shipitsyn

Institute of Metal Physics, Ural Division of the Russian Academy of Sciences, 620219 Ekaterinburg GSP-170, Russia

Received 9 December 1991, in final form 22 April 1992

Abstract. The Hubbard model in the limit of strong Coulomb interaction (the $(t$–$J)$ model) is studied by the diagram technique for Hubbard operators. The generalized random-phase approximation (GRPA) is formulated as an approximation taking into account electron loop-type diagrams. Within the framework of this approximation, both the dynamic magnetic and dielectric susceptibilities are calculated for a wide interval of electron concentrations, $0 < n < 1$. The magnetic susceptibility shows a crossover in the magnetic behaviour of the system from pure itinerant magnetism to magnetism with localized magnetic moments. The crossover occurs at a critical point, n_c, when the chemical potential for electrons of the lower Hubbard band changes sign. Magnetic phase diagrams are constructed on the $(t/U, n)$ plane at $T = 0$ for different types of crystal lattices. The behaviour of magnetic phases with temperature is also studied. The GRPA leads to a too drastic crossover, especially at low temperatures, because of insufficient allowance for the charge and spin fluctuations on a site. Summation of special diagram series shows that the Gaussian fluctuations of the effective electric and magnetic fields lead to a smoother picture of the crossover.

1. Introduction

Fundamental models for studying effects of electron correlations are the Hubbard model [1] and its limiting case—the $(t$–$J)$ model [2, 3]. In the past few years there has been a growing interest in these models owing to the idea of a possible non-phonon mechanism of high-T_c superconductivity in copper oxide compounds, which are strongly correlated systems [4]. However, investigations in this field are conducted mainly for two-dimensional models near the half-filling case. At the same time, the general problem of possible magnetic states in these models is very far from being resolved. One of the main goals of the theory should be to construct a phase diagram in the space of parameters $(t/U, n, T)$, where t and U enter in the Hubbard Hamiltonian

$$\hat{\mathcal{H}} = t \sum_{i\Delta\sigma} a^{+}_{i\sigma} a_{i+\Delta,\sigma} + U \sum_{i} n_{i\uparrow} n_{i\downarrow} \tag{1.1}$$

and n is the electron concentration, varying in the interval $0 < n < 1$. The edge of this interval, $n = 1$, corresponds to full filling of the lower Hubbard band and to a dielectric state with Néel-type antiferromagnetic order. Inside this interval, there are ferromagnetic (F) and antiferromagnetic (A) phases; however, the phase boundaries

0953-8984/92/499955+16$07.50

between them have not yet been defined reliably, because of the high complexity of the problem, especially in the situation with $U \sim t$ when a small parameter does not exist.

Two different limits are usually used to study the model described by Hamiltonian (1.1): $U \ll t$ and $U \gg t$ with successive extrapolations of the obtained results to the region $U \sim t$. In the first limiting case the following fundamental result was obtained many years ago for the dynamic magnetic susceptibility ($q = (\boldsymbol{q}, w)$) [5]:

$$\chi(q) = \chi_0(q)/[1 - U\chi_0(q)]. \tag{1.2}$$

This result corresponds to the random-phase approximation (RPA), an approximation where loop-type diagrams are summed. Here $\chi_0(q)$ is the Pauli-type magnetic susceptibility of a free-electron gas. Formula (1.2) underlies the description of the system's magnetic properties when the parameter U is not too large.

In the opposite limiting case ($U \gg t$), one usually passes from Hamiltonian (1.1) to the Hamiltonian of the (t–J) model by excluding states that are in the upper Hubbard band. The Hamiltonian of the (t–J) model is conveniently expressed in terms of the Hubbard operators, and a perturbation theory can be developed in the form of a diagram technique with Hubbard operators. Such a technique for the (t–J) model was constructed by us in [6]. This technique is a combination of the usual technique for Fermi systems [7] and the technique for spin operators [8].

In [6, 9] we proposed for the case $U \gg t$ the generalized random-phase approximation (GRPA) where all loop-type diagrams are summed similar to the case $U \ll t$. We calculated the magnetic susceptibility for the entire electron concentration interval, $0 < n < 1$. It turned out that a critical concentration, n_c, exists such that when $n < n_c$ the system behaves as an itinerant magnet, and when $n > n_c$ the system shows a dual behaviour in the sense that the magnetic susceptibility contains two contributions: a term that depends weakly on temperature (as for an itinerant magnet) and a term of the Curie type, $\sim 1/T$. The latter contribution shows that localized magnetic moments appear in the system. Thus, when the electron concentration is varied, a crossover from pure itinerant magnetism to magnetism with localized magnetic moments takes place. The existence of such a crossover indicates the power of the GRPA; however, the character of this crossover cannot be considered satisfactory, because the crossover is too sharp, especially at zero temperature. This means that the charge and spin fluctuations in the system have not been taken into account strictly enough in the GRPA approximation.

The aim of this paper is to study in detail the magnetic properties of the (t–J) model in terms of the GRPA in a wide interval of electron concentrations and also to make an attempt to go beyond the GRPA.

The paper is organized as follows. In section 2 a formalism based on the Hubbard operators is briefly described and the basic characteristics of the GRPA are formulated. In section 3 we calculate, within the framework of the GRPA, the Green functions describing the charge- and spin-density fluctuations and also the dynamic magnetic and dielectric susceptibilities. We conclude this section by presenting a phase diagram on the (t/U, n) plane at $T = 0$ for the simple cubic lattice. In section 4, in calculating the magnetic and dielectric susceptibilities, we take into account Gaussian fluctuations. It is shown that these fluctuations lead to a smoother crossover in the magnetic behaviour of the system with respect to electron concentrations. In section 5 we make an extensive study of magnetic phase diagrams for $T = 0$ on the basis of

the general expression for GRPA magnetic susceptibility. Section 6 discusses the limits of validity of the GRPA and also a number of important unsolved problems.

2. Generalized random-phase approximation

It is known [2, 3] that in the case of strong Coulomb repulsion ($U \gg t$) one can pass from the general Hamiltonian (1.1) to the Hamiltonian of the (t–J) model. In terms of Hubbard operators the Hamiltonian is given by the sum of three contributions [6, 9]:

$$\hat{\mathcal{H}} = \hat{\mathcal{H}}_0 + \hat{\mathcal{H}}_{\text{kin}} + \hat{\mathcal{H}}_{\text{eff}}$$

where

$$\hat{\mathcal{H}}_0 = \epsilon_+ \sum_i X_i^{++} + \epsilon_- \sum_i X_i^{--} \tag{2.1}$$

$$\hat{\mathcal{H}}_{\text{kin}} = t \sum_{i\Delta\sigma} X_i^{\sigma 0} X_{i+\Delta}^{0\sigma} \tag{2.2}$$

$$\hat{\mathcal{H}}_{\text{eff}} = J \sum_{i\Delta} (X_i^{-+} X_{i+\Delta}^{+-} - X_i^{++} X_{i+\Delta}^{--}) . \tag{2.3}$$

Here $\epsilon_\sigma = -\sigma h/2 - \mu$ is the energy of a one-electron state on a site (with μ being the chemical potential), $h = g\mu_B H$, H is the magnetic field and $J = t^2/U$ is the effective exchange integral.

In [6] we have developed a perturbation theory with respect to the Hamiltonian $\hat{\mathcal{H}}_{\text{int}} = \hat{\mathcal{H}}_{\text{kin}} + \hat{\mathcal{H}}_{\text{eff}}$ in the form of a diagram technique for Hubbard operators. The elements of this technique are fermion Green functions (full lines with white or black arrows denote spin projections), boson Green functions (broken lines with an arrow) and interactions (wavy and dotted lines for the quantities $\epsilon(k)$ and $J(k)$ respectively). These quantities are the coupling constants for the Hamiltonian $\hat{\mathcal{H}}_{\text{kin}}$ and $\hat{\mathcal{H}}_{\text{eff}}$.

In the same paper [6] we proposed a GRPA approximation that reduced essentially to the following statements:

(i) As a bare electron–electron vertex part, a set of three graphs is taken into account:

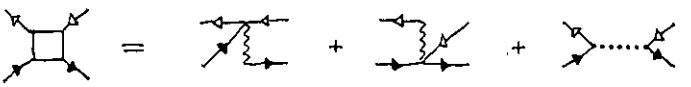

(2.4)

(ii) The effective electron–electron vertex part is found from the Bethe–Salpeter equation

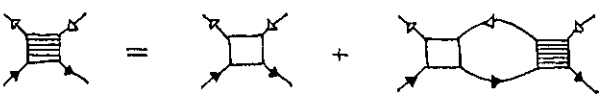

(2.5)

summing all diagrams with antiparallel ladders.

(iii) As a fermion Green function, the expression

$$G_\sigma(k) = 1/[i\omega_n - \xi_\sigma(k)] \qquad \xi_\uparrow(k) = \xi_\downarrow(k) = (1 - n/2)\epsilon(k) - \mu \tag{2.6}$$

is taken, which corresponds to the Hubbard-1 approximation in the paramagnetic phase.

Thus, the vertex part is determined by equation (2.5) and contains only loop-type diagrams, a circumstance that allows us to call this approximation a generalized RPA. It turns out that four types of loops exist:

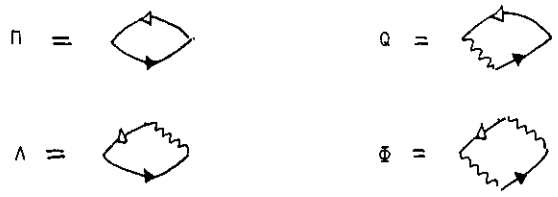

(2.7)

The analytical expressions corresponding to these loops (after summing over discrete frequencies) are

$$\begin{pmatrix} \Pi(k) \\ Q(k) \\ \Lambda(k) \\ \Phi(k) \end{pmatrix} = \frac{1}{N}\sum_{k_1} \begin{pmatrix} 1 \\ \epsilon(k_1) \\ \epsilon(k_1-k) \\ \epsilon(k_1)\epsilon(k_1-k) \end{pmatrix} \frac{f(\xi(k_1-k))-f(\xi(k_1))}{i\omega_n+\xi(k_1-k)-\xi(k_1)} \tag{2.8}$$

where $f(E)$ is the Fermi function.

By using the GRPA we calculated [6] the dynamic magnetic susceptibility of the $(t$–$J)$ model. The final result reads

$$\chi_s(k) = \chi_s^0(k)/\{[1-\Lambda(k)][1-Q(k)]+\chi_s^0(k)[\Phi(k)+J(k)]\}. \tag{2.9}$$

Here $\chi_s^0(k)$ is the bare susceptibility, which contains two terms

$$\chi_s^0(k) = \tfrac{1}{2}(nn_0/T)\delta_{\omega_n,0} - \Pi(k) \tag{2.10}$$

that correspond to the Curie-type susceptibility $\sim 1/T$ and the Pauli-type susceptibility depending weakly on temperature. Thus formulae (2.9) and (2.10) reflect a dualism in the magnetic behaviour of the system: the magnetic states are simultaneously itinerant and localized ones. The statistical weight of the localized states is determined by the factor

$$n^0 = 2e^{\mu/T}/(1+2e^{\mu/T}) \tag{2.11}$$

which depends on the chemical potential and temperature. The factor n^0 is a continuous function of μ/T at finite T, but when $T=0$

$$n^0 = \begin{cases} 1 & \mu > 0 \\ 0 & \mu < 0. \end{cases} \tag{2.12}$$

This means that when $\mu < 0$ a localized contribution to χ_s^0 is absent and the system behaves as an itinerant magnet. When $\mu > 0$ equation (2.10) tells us that localized magnetic moments appear although the Pauli-type term is also present. The chemical potential reverses sign when the electron concentration $n = n_c$ is equal to 2/3 in the Hubbard-1 approximation [6].

The Curie-type term in χ_s^0 is a quasi-static one because it is connected with the slow change in the direction of magnetic moment, while fluctuations of the value

of magnetic moment are chacterized by electron timescales. Thus formulae (2.9) and (2.10) reflect the following behaviour of the system. Fluctuations of the value of localized magnetic moment occur on each site of the lattice. Sometimes these fluctuations are long-lived, so a magnetic moment has enough time to change its direction before it decays. All such fluctuations are described by electron–electron loops (2.7).

The factor n^0 (2.12) describes a crossover of the system from pure itinerant behaviour to a localized one as the electron concentration is varied. Such a drastic change of n^0 is a result of a very crude approximation for the quantity

$$\partial(n_\uparrow - n_\downarrow)/\partial h|_{h\to 0} = (1/2T)n^0 \tag{2.13}$$

where $n_\sigma = \langle X^{\sigma\sigma}\rangle$ is the mean number of electrons with spin $\sigma = \uparrow, \downarrow$ on a site. Expression (2.11) for n^0 corresponds to the zero approximation of perturbation theory. Certainly, a crossover for the value n^0 should be smoother owing to spin and charge fluctuations on a site. Taking these into account is one of the problems solved in our paper.

3. Magnetic and dielectric susceptibilities of the paramagnetic phase

Let us introduce the Green functions of spin and charge fluctuations

$$D_s(g\tau, g'\tau') = \langle T(B_g^{+-}(\tau)B_{g'}^{+-}(\tau'))\rangle \tag{3.1}$$

$$D_c(g\tau, g'\tau') = \langle T(N_g(\tau)N_{g'}(\tau'))\rangle \tag{3.2}$$

where B_g^{+-} and N_g are the spin- and charge-density operators

$$B_g^{+-} = X_g^{++} - X_g^{--} \qquad N_g = X_g^{++} + X_g^{--}.$$

To calculate these functions, it is convenient to introduce the matrix function

$$D_{\sigma\sigma'}(g\tau, g'\tau') = \langle T(X_g^{\sigma\sigma}(\tau)X_{g'}^{\sigma'\sigma'}(\tau'))\rangle. \tag{3.3}$$

Corresponding to the $X^{\sigma\sigma}$ operators are two types of external vertices: a localized one (denoted by a thick dot) and an itinerant one (one electron line enters such a vertex and one electron line leaves it). Accordingly, the quantity (3.3) has a graphic representation whose structure is similar to that for the Green function of transverse spin components [6]. In matrix form this expression can be written as

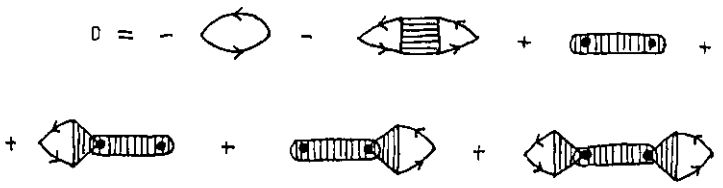

(3.4)

Each graph in this expression has two external vertices; the left-hand vertex corresponds to the operator $X^{\sigma\sigma}$ and the right-hand one corresponds to the operator

$X^{\sigma'\sigma'}$ in accordance with the definition (3.3). There are two types of external vertices: an itinerant and a localized one corresponding to the operators X^{++} and X^{--}:

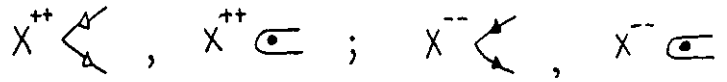

(3.5)

Localized vertices ●, corresponding to the X^{++} and X^{--} operators, are included in ovals; they are cumulants of the X-operator product averages. For example,

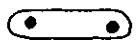

means the second-order cumulant for the average $\langle X^{\sigma\sigma} X^{\sigma'\sigma'} \rangle$.

Each graph element in (3.4) is a 2×2 matrix. For example, for zero-order graphs the following matrix notations are implied:

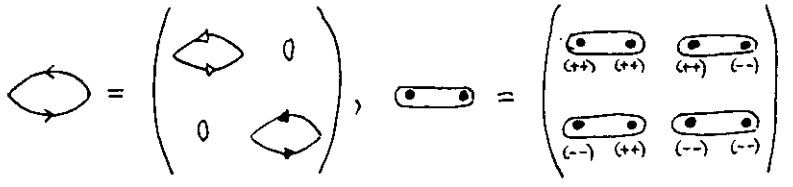

In the last expression $(++)$ or $(--)$ mean the operator X^{++} or X^{--}. Thus, rows and columns of the 2×2 matrix are enumerated here by complex indices $(++)$ and $(--)$. In expression (3.4) matrix summation over all intermediate indices is implied.

The four-point vertex parts in the GRPA are determined by a Bethe–Salpeter equation of type (2.5), but the three-point vertices are expressed in terms of the four-point vertices, as shown earlier [6].

Symbol

means a total cumulant, which is an infinite set of diagrams with two localized external vertices. This object in GRPA obeys the equation

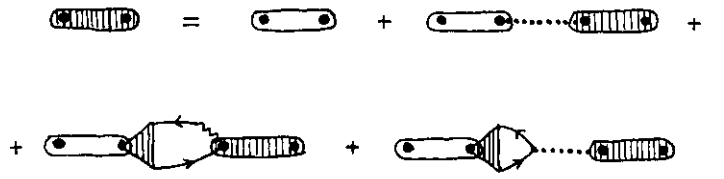

(3.6)

This equation takes into account all the graphs that are chains composed of bare cumulants linked by loops (2.7).

Solving equation (3.6) for

$K_{\sigma\sigma'}(k) =$ 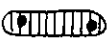

requires cumbersome calculations; however, the final result is wonderfully simple. We have in the paramagnetic phase

$$K_{++}(k) = \delta_{n0}\frac{1}{2T}\left(\frac{d_s^0(k)}{d_s(k)}\frac{\partial m^0}{\partial x_+} + \frac{d_c^0(k)}{d_c(k)}\frac{\partial n^0}{\partial x_+}\right)$$
$$K_{+-}(k) = -\delta_{n0}\frac{1}{2T}\left(\frac{d_s^0(k)}{d_s(k)}\frac{\partial m^0}{\partial x_+} - \frac{d_c^0(k)}{d_c(k)}\frac{\partial n^0}{\partial x_+}\right). \tag{3.7}$$

Here d_s^0, d_c^0, d_s and d_c are expressed in terms of the quantities corresponding to the loop diagrams (2.7):

$$d_s^0 = (1-\Lambda)(1-Q) - \Pi(\Phi + J) \qquad d_c^0 = (1+\Lambda)(1+Q) - \Pi(\Phi - J) \tag{3.8}$$

$$d_s = d_s^0 + \delta_{n0}\frac{1}{T}\frac{\partial m^0}{\partial x_+}(\Phi + J) \qquad d_c = d_c^0 + \delta_{n0}\frac{1}{T}\frac{\partial n^0}{\partial x_+}(\Phi - J). \tag{3.9}$$

The quantities $\partial m^0/\partial x_+$ and $\partial n^0/\partial x_+$ are cumulants of the zero approximation. They are composed of the operators $X^{\sigma\sigma}$. In accordance with the zero-approximation Hamiltonian (2.1), the cumulants are calculated with the help of the generating functional

$$W = \mathrm{Sp}\left(\exp(x_+X^{++} + x_-X^{--})\right) \qquad x_+ = -\epsilon_+/T, x_- = -\epsilon_-/T$$

by the formula

$$\langle X^{\sigma_1\sigma_1}\dots X^{\sigma_n\sigma_n}\rangle_0 = (1/W)\partial^n W/\partial x_{\sigma_1}\dots\partial x_{\sigma_n}.$$

In expressions (3.7) and (3.9)

$$m^0 = n_+^0 - n_-^0 \qquad n^0 = n_+^0 + n_-^0$$

where

$$n_\sigma^0 = \langle X^{\sigma\sigma}\rangle_0 = \mathrm{e}^{x_\sigma}/(1 + \mathrm{e}^{x_+} + \mathrm{e}^{x_-}). \tag{3.10}$$

For the paramagnetic phase we obtain at $h = 0$

$$\partial m^0/\partial x_+ = \tfrac{1}{2}n^0 \qquad \partial n^0/\partial x_+ = \tfrac{1}{2}n^0(1-n^0) \tag{3.11}$$

where n^0 is given by (2.11).

We now present the final result of our calculation of the Green functions $D_{\sigma\sigma'}$ with the help of the graphical expression (3.4). Similar calculations have been done for the transverse spin Green function in [6], to which we refer the reader for details. Thus,

$$D_{++}(k) = \frac{1}{2d_s(k)}\left(\delta_{n0}\frac{1}{T}\frac{\partial m^0}{\partial x_+} - \Pi\right) + \frac{1}{2d_c(k)}\left(\delta_{n0}\frac{1}{T}\frac{\partial n^0}{\partial x_+} - \Pi\right)$$
$$D_{+-}(k) = -\frac{1}{2d_s(k)}\left(\delta_{n0}\frac{1}{T}\frac{\partial m^0}{\partial x_+} - \Pi\right) + \frac{1}{2d_c(k)}\left(\delta_{n0}\frac{1}{T}\frac{\partial n^0}{\partial x_+} - \Pi\right).$$

Now, using the definitions (3.1) and (3.2), we write the final results for magnetic and dielectric susceptibilities:

$$\tfrac{1}{2}D_s(k) = \chi_s^0(k)/\{[1-\Lambda(k)][1-Q(k)] + \chi_s^0(k)[\Phi(k)+J(k)]\} \tag{3.12}$$

$$\tfrac{1}{2}D_c(k) = \chi_c^0(k)/\{[1+\Lambda(k)][1+Q(k)] + \chi_c^0(k)[\Phi(k)-J(k)]\}. \tag{3.13}$$

Here χ_s^0 and χ_c^0 are bare susceptibilities

$$\chi_s^0 = (1/T)(\partial m^0/\partial x_+)\delta_{n0} - \Pi \tag{3.14}$$

$$\chi_c^0 = (1/T)(\partial n^0/\partial x_+)\delta_{n0} - \Pi. \tag{3.15}$$

The expression (3.12) for the magnetic susceptibility coincides with the expression (2.9), which we calculated with the help of the spin Green function for transverse components [6]. This coincidence should take place for the paramagnetic phase. In [6] we studied, on the basis of expression (2.9) for $\chi_s(k,0)$, the instabilities of the paramagnetic phase with respect to the occurrence of a magnetic order with the wavevectors $k = 0$ and $k = k_0$, where $k_0 = (\pi,\pi,\pi)$ is the wavevector of antiferromagnetism. To calculate the fundamental quantities Π, Λ, Q and Φ we took a model with constant density of states. In figure 1 we present results of a similar calculation for the simple cubic lattice. The boundaries of F and A instabilities remain qualitatively the same as those for a model with constant density of states. Ferromagnetism arises when the electron concentration exceeds some critical concentration $n_c = 2/3$. The region of antiferromagnetism adjoins the region of $n \lesssim 1$ and broadens as the parameter t/U increases, that is, with increasing effective exchange interaction t^2/U.

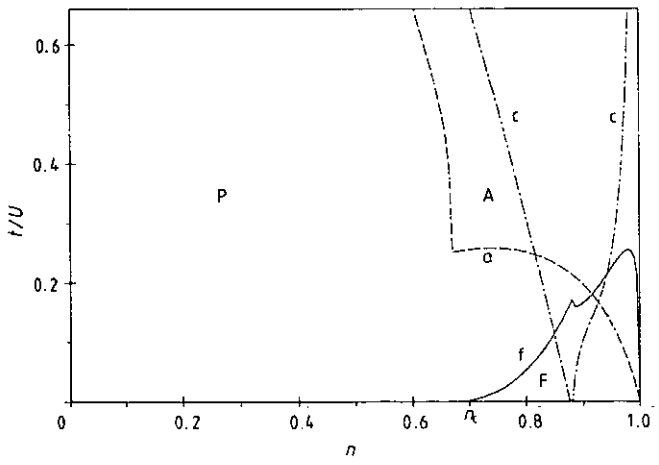

Figure 1. Phase diagram for the simple cubic lattice at $T = 0$; curves f, a and c are boundaries of F, A and dielectric instabilities of the paramagnetic phase.

The lines of magnetic instabilities are determined by the zeros of the denominator in expression (3.12) for the magnetic susceptibility at zero frequency. The zeros of the denominator of the dielectric susceptibility determine the curves c in figure 1. The system turns out to be unstable with respect to dielectric ordering with $k = 0$ in the sector lying between the c curves. However, the greater part of the unstable region

coincides with the region of magnetically ordered states, while the formula (3.15) is valid only for the paramagnetic state. Because of that, the region of dielectric instability is rather small.

In figure 1 one can see some overlap of the regions of instability of the paramagnetic phase with respect to F or A ordering. To determine the genuine states of the system in each part of the $(t/U, n)$ plane, it is necessary to compare the total energies of these phases.

At the point n_c the chemical potential in the lower Hubbard band changes sign. This fact leads to the above-mentioned drastic change in the quantity n^0 (2.11), a change that indicates that localized magnetic moments appear in the system at $n > n_c$.

4. Allowance for the Gaussian fluctuation

In the zero approximation, the expression (2.11) for n^0 gives too drastic a change in the system's magnetic properties with varying electron concentration. To get a smoother behaviour, it is necessary to dress thicken the bare cumulant

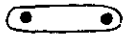

involved in equation (3.6). The dressing is possible by including into the bare cumulant different graphical structures that contain vertices $X^{\sigma\sigma}$. Multiple inclusion of single-vertex structures leads only to a shift of the chemical potential in the expression for the zero-approximation cumulant and is, therefore, not essential. One has to include graphical structures with two vertices at least.

Let us consider the series

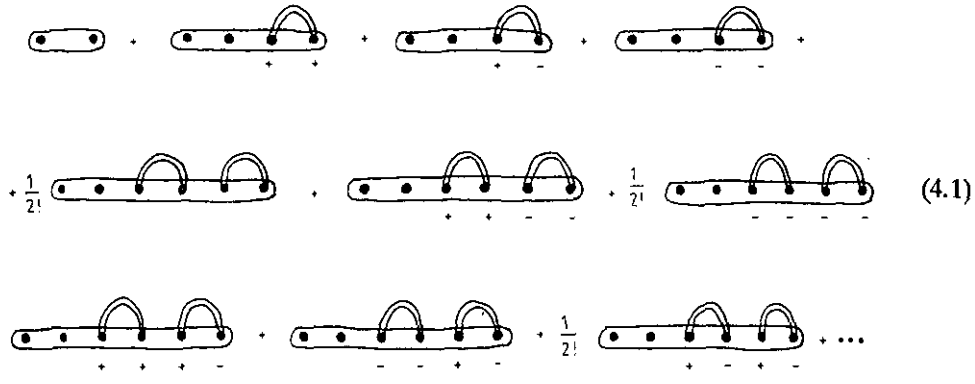

(4.1)

where two-point structures with vertices X^{++} and X^{--} of all possible combinations are included. We shall calculate these structures in GRPA. This means that the graphs composed of loops (2.7) must be summed. It can be readily verified that all of these graphs are contained in the graphical expression

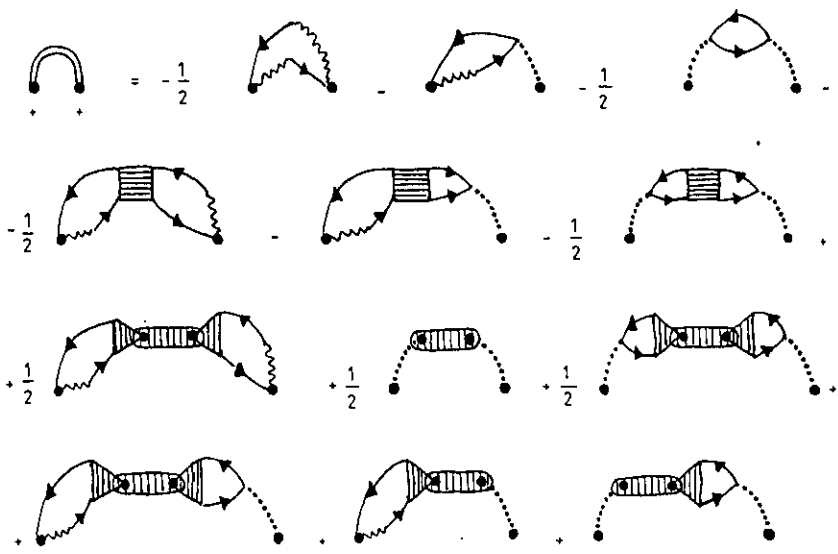

(4.2)

A similar expression can be written for other two-point structures characterized by the vertices X^{++} and X^{--}.

Denote the quantity (4.2) as $I_{++}(k)$ and the associated quantity as $I_{+-}(k)$. Very complicated calculations lead, however, to rather simple and clear answers:

$$I_{++}(k) = -\tfrac{1}{4}(\Phi + J)/d_s - \tfrac{1}{4}(\Phi - J)/d_c \qquad I_{--}(k) = I_{++}(k) \tag{4.3}$$

$$I_{+-}(k) = \tfrac{1}{2}(\Phi + J)/d_s - \tfrac{1}{2}(\Phi - J)/d_c. \tag{4.4}$$

These quantities allow one to calculate the two-point structures inserted in cumulants of the series (4.1). These structures correspond to the expressions

$$\frac{1}{T}\frac{1}{N}\sum_{k} I_{++}(k,0) \qquad \frac{1}{T}\frac{1}{N}\sum_{k} I_{+-}(k,0).$$

Let us write the series (4.1) in analytical form. We denote the bare cumulant as a function of two variables $f(x_+, x_-)$. If we pass on to the new variables

$$x = \tfrac{1}{2}(x_+ + x_-) = \mu/T \qquad y = \tfrac{1}{2}(x_+ - x_-) = \tfrac{1}{2}h/T \tag{4.5}$$

the series (4.1) can be represented as the following Taylor series:

$$f(x,y) + \frac{\Delta x}{4}\frac{\partial^2 f}{\partial x^2} + \frac{\Delta y}{4}\frac{\partial^2 f}{\partial y^2} + \frac{1}{2!}\left[\left(\frac{\Delta x}{4}\right)^2 \frac{\partial^4 f}{\partial x^4} + 2\left(\frac{\Delta x}{4}\frac{\Delta y}{4}\right)\frac{\partial^4 f}{\partial x^2 \partial y^4} + \left(\frac{\Delta y}{4}\right)^2 \frac{\partial^4 f}{\partial y^4}\right] + \cdots \tag{4.6}$$

It is easy to see that the general term of this series is $(1/n!)(\Delta z/4)^n \partial^{2n} f/\partial z^{2n}$. The total sum of the series reduces to the expression

$$\frac{1}{\pi(\Delta x \Delta y)^{1/2}} \int_{-\infty}^{+\infty} d\xi \int_{-\infty}^{+\infty} d\eta \exp\left[-\left(\frac{\xi^2}{\Delta x} + \frac{\eta^2}{\Delta y}\right)\right] f(x+\xi, y+\eta) \tag{4.7}$$

which can be interpreted as averaging $f(x,y)$ over the Gaussian fluctuations of the fields x and y with Δx and Δy as dispersions of the Gaussian fluctuations. Here

$$\Delta y = -\frac{1}{T}\frac{1}{N}\sum_{k}\frac{\Phi(k_1 0)+J(k)}{d_s(k,0)} \equiv \frac{1}{T}\frac{1}{N}\sum_{k} V_s(k,0) \tag{4.8}$$

$$\Delta x = -\frac{1}{T}\frac{1}{N}\sum_{k}\frac{\Phi(k,0)-J(k)}{d_c(k,0)} \equiv \frac{1}{T}\frac{1}{N}\sum_{k} V_c(k,0). \tag{4.9}$$

As a result of summing the graphical series, the quantities $\partial m^0/\partial x_+$ and $\partial n^0/\partial x_+$ in formulae (3.14) and (3.15), corresponding to the second-order cumulants, are renormalized to $\widetilde{\partial m^0/\partial x_+}$ and $\widetilde{\partial n^0/\partial x_+}$. Taking into account the explicit expressions

$$m^0(x_+,x_-) = \frac{e^{x_+}-e^{x_-}}{1+e^{x_+}+e^{x_-}} \qquad n^0(x_+,x_-) = \frac{e^{x_+}+e^{x_-}}{1+e^{x_+}+e^{x_-}}$$

we can represent them as

$$\widetilde{\frac{\partial m^0}{\partial x_+}} = \frac{1}{\pi(\Delta x\Delta y)^{1/2}}\int_{-\infty}^{+\infty} d\xi \int_{-\infty}^{+\infty} d\eta \times \exp\left[-\left((\xi^2/\Delta x)+(\eta^2/\Delta y)\right)\right] n^0(x+\xi,\eta)\tanh'(\eta) \tag{4.10}$$

$$\widetilde{\frac{\partial n^0}{\partial x_+}} = \frac{1}{\pi(\Delta x\Delta y)^{1/2}}\int_{-\infty}^{+\infty} d\xi \int_{-\infty}^{+\infty} d\eta \exp\left[-\left((\xi^2/\Delta x)+(\eta^2/\Delta y)\right)\right] \times n^0(x+\xi,\eta)[1-n^0(x+\xi,\eta)] \tag{4.11}$$

(the external magnetic field is equal to zero). Here

$$n^0(x+\xi,\eta) = 2\cosh\eta\, e^{x+\xi}/(1+2\cosh\eta\, e^{x+\xi}). \tag{4.12}$$

From expressions (4.10) and (4.11), one can see that ξ and η are actually electric and magnetic field fluctuations created by charge- and spin-density fluctuations. The measures of the intensity of these fluctuations (dispersions of the Gaussian distribution), Δx and Δy, are expressed, according to formulae (4.8) and (4.9), through the effective interactions v_c and v_s of charge and spin degrees of freedom. Because the expressions (4.8) and (4.9) contain a summation over momentum, the quantities Δx and Δy are measures of the effective zero-frequency self-interactions on a site, which are divided by the average value of the heat motion energy kT. Note that our theory of Gaussian fluctuations in the $(t$–$J)$ model is completely similar to the situation in the Ising model, where spin fluctuations have been taken into account for the first time by summing graphical series for cumulants [8].

Consider in detail the expression (4.10). If Δx is small ($\Delta x \ll \Delta y$), an integral over ξ is taken, and we get

$$\widetilde{\frac{\partial m^0}{\partial x_+}} = \frac{1}{(\pi\Delta y)^{1/2}}\int_{-\infty}^{\infty} d\eta \exp(-\eta^2/\Delta y)\frac{2e^x}{1+2\cosh\eta\, e^x}\frac{1}{\cosh\eta}. \tag{4.13}$$

This expression is meaningful when $\Delta y > 0$. If it turns out that $\Delta y < 0$, summing the series (4.6) leads to the formula (4.7), where one has to make the replacement

$$f(x+\xi, y+\eta) \to f(x+\xi, y+\mathrm{i}\eta).$$

In particular for the case $\Delta x \to 0$ we have, instead of formula (4.13), the expression

$$\widetilde{\frac{\partial m^0}{\partial x_+}} = \frac{1}{(\pi\Delta y)^{1/2}} \int_{-\infty}^{\infty} \mathrm{d}\eta \exp(-\eta^2/|\Delta y|) \frac{2\mathrm{e}^x}{1+2\mathrm{e}^x \cos\eta} \frac{1}{\cos\eta} \qquad (4.14)$$

which diverges in the limit $x \to \infty$. This indicates that, at low temeprature and $n > n_c$, spin fluctuations are very strong and cannot be treated as Gaussian ones; it is necessary to take into account the interaction of these fluctuations.

Similarly, one can consider the limit of small Δx in the expression (4.11) and also the limit of small Δy in both (4.10) and (4.11). The results of a numerical calculation of the one-dimensional integrals obtained from expressions (4.10) and (4.11) on integrating over ξ (when $\Delta x \to 0$) and over η (when $\Delta y \to 0$) are presented in figures 2 and 3. There, the behaviour of the quantities $\widetilde{\partial m^0/\partial x_+}$ and $\widetilde{\partial n^0/\partial x_+}$ is given as a function of the quantities Δx and Δy characterizing the intensity of the charge and spin fluctuations at any value of parameter x. From figure 2, one can see the behaviour of the localized magnetic moment with varying x. With increasing Δx the drastic crossover from itinerant to localized magnetism is smeared. Figure 3 shows the change of $\widetilde{\partial n^0/\partial x_+}$, which determines the value of the localized electric moment arising in the vicinity of the point $x = 0$, where the chemical potential changes sign.

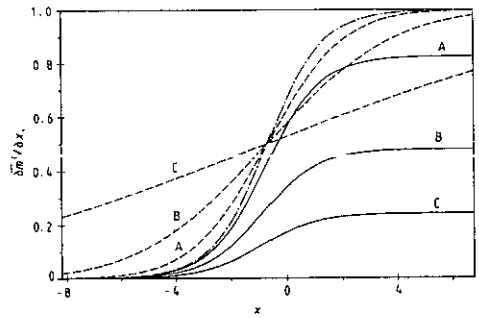

Figure 2. Plot of $\widetilde{\partial m^0/\partial x_+}$ as a function of x with different values of spin and charge fluctuations: chain curve, $\Delta x = 0$, $\Delta y = 0$; full curves, $\Delta x = 0$, $\Delta y = 0.5$ (A), $\Delta y = 4$ (B), $\Delta y = 20$ (C); broken curves, $\Delta y = 0$, $\Delta x = 4$ (A), $\Delta x = 20$ (B), $\Delta x = 200$ (C).

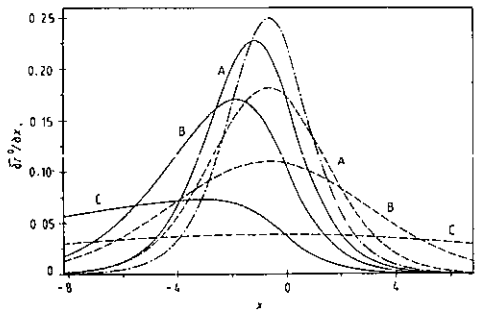

Figure 3. Plot of $\widetilde{\partial n^0/\partial x_+}$ as a function of x with different values of spin and charge fluctuations: chain curve, $\Delta x = 0$, $\Delta y = 0$; full curves, $\Delta x = 0$, $\Delta y = 4$ (A), $\Delta y = 20$ (B), $\Delta y = 200$ (C); broken curves, $\Delta y = 0$, $\Delta x = 4$ (A), $\Delta x = 20$ (B), $\Delta x = 200$ (C).

Thus fluctuation of charge and spin on a site leads to smearing of the features of the quantities $\widetilde{\partial m^0/\partial x_+}$ and $\widetilde{\partial n^0/\partial x_+}$ (corresponding to the mean-field approximation) as functions of the parameter x. Determining the electron-concentration and temperature dependences of the quantities $\widetilde{\partial m^0/\partial x_+}$ and

$\widetilde{\partial n^0/\partial x_+}$ is a complicated problem, because the fluctuation parameters Δx and Δy depend on μ and T. These parameters are determined by expressions (4.8) and (4.9).

5. Magnetic phase diagrams of the model

In this section, we discuss in greater detail the system's magnetic properties, which one can derive from the general expression (2.9) for the magnetic susceptibility. The phase diagram for the simple cubic lattice at $T = 0$ has been shown in figure 1. A calculation for the body-centred cubic lattice (and also for the constant density-of-states model) shows that the curves restricting the regions of the F and A phases do not change very much, so the type of magnetic phase diagram remains qualitatively the same for different lattices.

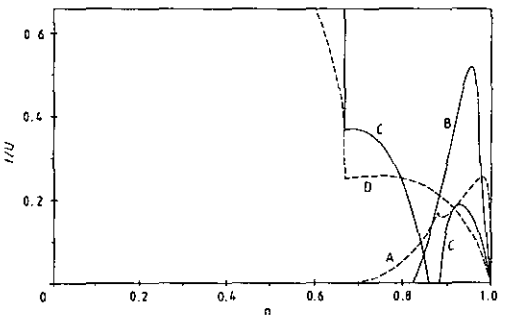

Figure 4. Phase diagram for the simple cubic lattice at $T = 0$ with different antiferromagnetic structures: A, $\boldsymbol{k} = (0, 0, 0)$; B, $\boldsymbol{k} = (0, 0, \pi)$; C, $\boldsymbol{k} = (0, \pi, \pi)$; D, $\boldsymbol{k} = (\pi, \pi, \pi)$.

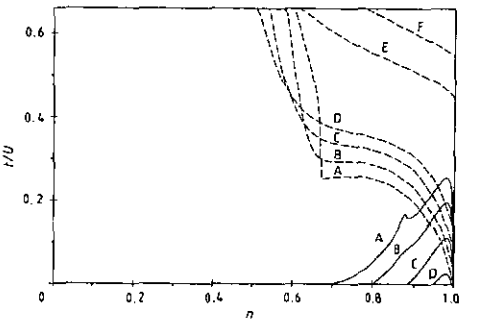

Figure 5. Phase diagram for the simple cubic lattice at finite temperatures (full and broken curves are boundaries of F and A phases): A, $T/6t = 0$; B, $T/6t = 0.015$; C, $T/6t = 0.035$; D, $T/6t = 0.055$; E, $T/6t = 0.21$; F, $T/6t = 0.28$.

Further, we consider again the simple cubic lattice. In figure 1 the region of A instability with wavevector $\boldsymbol{k} = \boldsymbol{k}_0 = (\pi, \pi, \pi)$ was shown. In addition to this instability, figure 4 shows also curves of instability with respect to different antiferromagnetic phases. One can see an interesting tendency. There are two intermediate structures with wavevectors $(0, 0, \pi)$ and $(0, \pi, \pi)$. The regions of instabilities with respect to these structures adjoin the regions of the F and A phases respectively. That is, the more ferromagnetic planes there are in an antiferromagnetic structure, the closer the structure is to the F phase; and the fewer ferromagnetic planes, the closer the structure is to the A phase. It can also be shown that the paramagnetic phase is unstable with respect to long-wave modulations of an antiferromagnetic phase with $\boldsymbol{k} = \boldsymbol{k}_0$ and of a ferromagnetic phase. The regions of these instabilities are close to the boundaries of the A and F phases, so we do not present the corresponding phase diagram.

The results of our study of the model at finite temperatures are shown in figures 5 and 6. From figure 5, one can see that with increasing T the regions of magnetic phases reduce in area. Finally, figure 6 shows the temperature dependence of inverse magnetic susceptibility. When the temperature is high enough, $\chi^{-1} = T$, as in

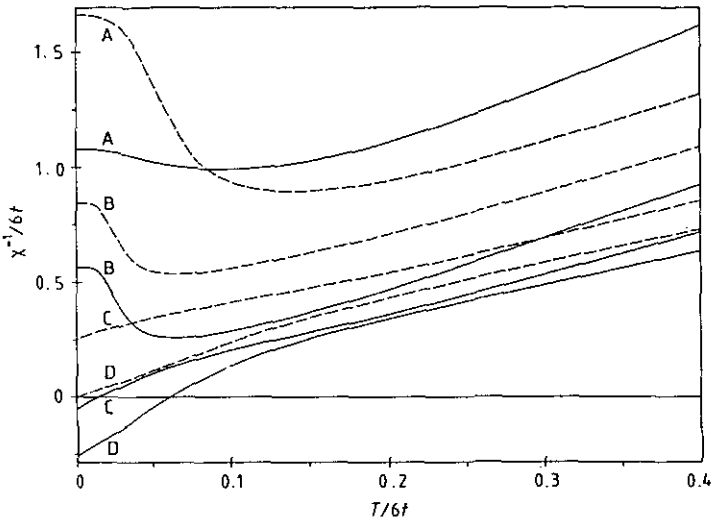

Figure 6. Temperature dependence of inverse magnetic susceptibility for the simple cubic lattice at $t/U = 0$ with different values of electron concentration. Full curves, $\boldsymbol{k} = (0, 0, 0)$: A, $n = 0.2$, B, $n = 0.55$, C, $n = 0.8$, D, $n = 0.98$. Broken curves, $\boldsymbol{k} = (\pi, \pi, \pi)$: A, $n = 0.4$, B, $n = 0.55$, C, $n = 0.8$, D, $n = 1.0$.

the case of non-interacting localized magnetic moments. At low temperatures the behaviour of χ^{-1} depends on n. When $n < n_c$ the curves are concave; when $n > n_c$ the curves are convex. Note that a similar temperature behaviour of inverse susceptibility was obtained in [10], where the two-loop approximation was used for calculating the thermodynamic potential. Such behaviour of χ^{-1} at $n > n_c$ is specific to strongly correlated systems. Particularly, it was revealed in the double-exchange model (s–d model in the strong s–d exchange interaction limit) [11].

6. Conclusions

In this paper and also in a previous paper [6], we investigated the magnetic properties of the $(t$–$J)$ model with the help of the GRPA approximation. In two other papers [12, 13] we used the same approximation in analysing the possibility of superconducting pairing via the interaction of electrons with spin fluctuations in the $(t$–$J)$ model.

As to magnetism, the most interesting result of the GRPA, in our view, is the occurrence of a crossover from pure itinerant to localized magnetism as the electron concentration is varied. Support for this comes from the fact that a Curie-type contribution arises in the magnetic susceptibility that is proportional to $1/T$. Originally [6], this crossover was too drastic; at $T = 0$ it took place at one point $n = n_c$, where the chemical potential in the lower Hubbard band changes sign. In this paper we have shown that allowance for only Gaussian fluctuations of magnetic and electric effective fields leads to smearing of this crossover. More accurate allowance for fluctuations permits one to expect a still smoother crossover, which is more reasonable from physical considerations. Studying this problem further is very important.

We propose that localized magnetic moments in a system with $U \gg t$ exist because of a Curie-type contribution to the magnetic susceptibility. In the technique with Hubbard operators such a term appears in a very simple and natural way, by contrast with theories starting from the opposite limit $U \ll t$ [14]. In the theories of

strongly correlated systems that exploit the slave boson technique, obtaining a Curie-type contribution to the magnetic susceptibility is also a difficult problem. Specifically, in [15] the Curie term in χ_s^0 is absent.

The magnetic susceptibility is, however, an integral characteristic of the system. It would be interesting to study local characteristics such as

$$\frac{1}{N}\sum_{\boldsymbol{k}}\chi_s(\boldsymbol{k},0) \qquad \frac{T}{N}\sum_{k}\chi_s(\boldsymbol{k},i\omega_n). \tag{6.1}$$

The first characteristic is the spectral density of a spin correlator; the second one is the magnitude of a localized magnetic moment. Inspection of expression (2.9) for the magnetic susceptibility shows that the evaluation of expressions (6.1) calls for numerical calculations and has not yet been done. It would be interesting also to calculate, with the help of the local spectral density $(1/N)\sum \boldsymbol{k}\chi_s(\boldsymbol{k},0)$ the mean lifetime τ_s of a localized magnetic moment and the evolution of a magnetic moment with varying electron concentration. We expect that at point $n = n_c$ a crossover of the quantity τ_s would take place from the electron timescale $\hbar/t$ to a larger scale that exceeds the spin correlation timescale $\hbar/J$. This problem is especially important in the limit $U \to \infty$. Note also the importance of exploring the sum rule for spin correlators calculated in the GRPA.

We now discuss the range of applicability of the GRPA. Similar to the RPA in the theory of systems with $U \ll t$, the GRPA for strongly correlated systems $U \gg t$ does not use explicitly any small parameter. In both cases loop-type diagrams are summed. A formal argument for that could be the large number of degenerate electron states f, because a loop contains a trace along the discrete indices characterizing the electron states and has a factor f. Clearly, if f were large one would need to sum the graphs containing the maximal number of such loops. Because in our case $f = 2$ (two spin projections) a large parameter does not exist, the results of both the GRPA and the RPA are interpolative in character.

At the same time it is well known that RPA theories, for example formula (1.2) for the magnetic susceptibility, provide a good description of many properties of the system in a large interval of parameters. We hope also that, for strongly correlated systems, the GRPA theory gives a correct description of systems in a wide concentration interval $0 < n < 1$. Recall that one of the most fundamental results of the GRPA theory is the description of the crossover from itinerant to localized magnetism.

At the edges of this interval the GRPA should not give an adequate physical picture for two reasons at least. First, as electron states for the zero approximation we take the Hubbard-I approximation. Near the half-filling limit ($n = 1$), this approximation is poor. The physical picture near this limit corresponds to a magnetic polaron or a quasi-oscillator [16], that is, a hole that moves in an antiferromagnetic matrix. Secondly, the idea that fermion states are coherent quasi-particles of the Fermi liquid is questionable [17]. As the latest review of this problem, we can mention [18]. Thus the regions $n \ll 1$ and $1 - n \ll 1$ must be excluded from the electron concentration interval where the GRPA can give an adequate description of strongly correlated systems. However, small parameters (electron or hole concentrations) exist for these regions. It is known that in these situations one has to sum a series of ladder-type diagrams rather than loop-type diagrams [19, 20]. Such approaches to the theory of strongly correlated systems will be developed in a subsequent paper.

References

[1] Hubbard J 1963 *Proc. R. Soc.* A **276** 238
[2] Harris A V and Lange R V 1967 *Phys. Rev.* **157** 295
[3] Hirsch J E 1985 *Phys. Rev. Lett.* **54** 1317
[4] Anderson P W 1987 *Science* **235** 1196
[5] Izuyama T, Kim D and Kubo R 1963 *J. Phys. Soc. Japan* **18** 1025
[6] Izyumov Yu A and Letfulov B M 1990 *J. Phys.: Condens. Matter* **2** 8905
[7] Abrikosov A A, Gorkov L P and Dzyaloshinski I E 1975 *Methods of Quantum Field Theory in Statistical Physics* (New York: Dover)
[8] Izyumov Yu A and Scryabin Yu N 1988 *Statistical Mechanics of Magnetically Ordered Systems* (New York: Consultants Bureau)
[9] Izyumov Yu A and Letfulov B M 1991 *J. Phys.: Condens. Matter* **3** 5373
[10] Letfulov B M 1989 *Teor. Mat. Fiz.* **12** 434
[11] Anderson P W and Hasegawa H 1955 *Phys. Rev.* **100** 675
[12] Izyumov Yu A and Letfulov B M 1991 *Europhys. Lett.* **16** 497
[13] Izyumov Yu A and Letfulov B M 1991 *Int. J. Mod. Phys.* B in press
[14] Moriya T 1985 *Spin Fluctuations in Itinerant Electron Magnetism* (Berlin: Springer)
[15] Tanamoto T, Kuboki K and Fukuyama H 1991 Magnetic Properties of (t–J) Model *Technical Report* Ser. AN 2421
[16] Bulaevski L N, Nagaev E L and Khomski D I 1968 *Sov. Phys.–JETP* **54** 1562
[17] Brinkman W F and Rice T M 1970 *Phys. Rev.* B **2** 1324
[18] Izyumov Yu A 1991 *Sov. Usp.* **161** 2
[19] Kanamori J 1963 *Prog. Theor. Phys.* **30** 276
[20] Nagaoka Y 1966 *Phys. Rev.* **147** 392